Article

Selective Oxidation of Raw Glycerol Using Supported AuPd Nanoparticles

Carine E. Chan-Thaw [1], Sebastiano Campisi [1], Di Wang [2], Laura Prati [1] and Alberto Villa [1,*]

[1] Dipartimento di Chimica, Università degli Studi di Milano, via Golgi 19, I-20133 Milano, Italy;
E-Mails: carine.chanthaw@unimi.it (C.E.C.-T.); sebastiano.campisi@unimi.it (S.C.);
laura.prati@unimi.it (L.P.)

[2] Institut für Nanotechnologie, Forschungszentrum Karlsruhe in der Helmholtz-Gemeinschaft
Hermann-von-Helmholtz-Platz 1, 76344 Eggenstein-Leopoldshafen, Germany;
E-Mail: di.wang@kit.edu

* Author to whom correspondence should be addressed; E-Mail: alberto.villa@unimi.it;
Tel.: +39-250-314-361.

Academic Editor: Keith Hohn

Abstract: Bimetallic AuPd supported on different carbonaceous materials and TiO_2 was tested in the liquid phase oxidation of commercial grade and raw glycerol. The latter was directly obtained from the base-catalyzed transesterification of edible rapeseed oil using KOH. The best catalytic results were obtained using activated carbon and nitrogen-functionalized carbon nanofibers as supports. In fact, the catalysts were more active using pure glycerol instead of the one obtained from rapeseed, where strong deactivation phenomena were present. Fourier transform infrared (FT-IR) and TEM were utilized to investigate the possible reasons for the observed loss of activity.

Keywords: raw glycerol; AuPd; liquid phase oxidation

1. Introduction

The use of biomass for the production of renewable raw materials and their conversion to high value chemicals is still a young field, but a significant potential has been shown [1]. Only 3.5% of the existing biomass production is presently being used for human needs. Most of this is used for human

food (around 62%), 33% for energy use, paper and construction needs, and the remaining 5% is used for clothing, detergents and chemicals. The other 96.5% of the biomass production is used in the planetary ecosystem. A recent EU directive (2009/28/EC) has set the target of achieving, by 2020, a 20% share of energy from renewable energy sources in the EU's overall energy consumption. In this context, special consideration is paid to the role played by the use of waste oils or non-edible vegetable oils as feedstock that do not interfere with the food chain.

Vegetable oils are composed of triglycerides, and their transesterification results in obtaining three moles of fatty acid methyl esters (FAMEs) and one mole of glycerol. The products of the hydrogenation of these FAMEs can be used as biodiesel or as non-negligible products, such as lubricants [2], surfactants, solvents [3], polymers and fine chemicals [4]. The tremendous growth of the biodiesel industry has concomitantly been accompanied by an over-production of raw glycerol [5,6]. Together with the high cost of disposal, this unused product was often released into landfills. Therefore, from an economical and environmental aspect, it is worthwhile to focusing on this raw product. The valorization of a huge amount of compound that is considered as waste, hence being low cost, would significantly affect the price of biodiesel. For this reason, since the end of the 20th century, intensive research has been focused on the use of glycerol as a benign solvent [7] or as starting material for subsequent transformations [8–15]. However, nearly almost all results that can be found in the literature were obtained with pure commercial glycerol, whereas few reports used raw glycerol as a starting material [16–18].

Crude glycerol is normally obtained by a simple transesterification reaction of vegetable oils with methanol using sodium (Na) or potassium (K) hydroxide as catalysts. These ions together with the alcohol or the remaining free fatty acids represent the main impurities that could thus deposit on the active sites on the catalyst surface or modify any pre-established reaction pathway, during the subsequent transformations of glycerol. Skrzyńska *et al.* recently reported on the potential behavior of crude glycerol impurities at various pH in liquid phase oxidation [18]. Konaka *et al.* [19] intentionally prepared a potassium-supported zirconia-iron oxide catalyst for crude glycerol conversion into allyl alcohol. A proper amount of K, in their case 5 mol%, successfully produced allyl alcohol, a useful chemical for the preparation of resins, paints and plasticizers [20]. An amount of K over the mentioned value is detrimental for the reaction. Therefore, the composition of the crude oil could influence any catalytic transformation. Among the possible routes for glycerol valorization, selective oxidation is of importance, because glycerol acts as a platform molecule that is convertible through the use of inexpensive oxidizing agents (air, oxygen, H_2O_2, *etc.*) in a variety of value-added derivatives (glyceric acid, tartronic acid, hydroxypyruvic acid, *etc.*).

Since Prati *et al.* have demonstrated that gold supported on activated carbon (AC) in the presence of a base was catalytically active and selective for the oxidation of ethylene glycol to produce glycolate [9], gold as a catalyst for liquid phase oxidation of alcohols has been the subject of many studies [21–23]. In particular, gold catalysts were shown to be more resistant to oxygen poisoning and selective for the oxidation of primary alcohols. In order to increase the catalytic performance of gold catalyst, the support effect, as well as the introduction of a second metal has been deeply investigated. It was shown that alloying Pd to Au nanoparticles leads to a significant enhancement of the catalytic activity in the selective oxidation of glycerol, also increasing the durability of the catalyst [24–26]. On

the other hand, the choice of the support has a strong influence on the catalytic activity of the Au catalyst [27,28].

Indeed, the support has the role of avoiding coalescence and agglomeration of metal nanoparticles by reducing their mobility. In many cases, the strong metal-support interactions (SMSI) can also play a non-negligible role in the reaction mechanism. Furthermore, the surface properties of the catalysts (acidity, hydrophobicity/hydrophilicity, *etc.*) are principally determined by the support [28].

Herein, we investigate the catalytic performance of supported AuPd catalysts, prepared by sol immobilization, in the selective oxidation of both commercial glycerol and that directly obtained from the transesterification of rapeseed oil. To study the support effect, carbonaceous materials having different textural and surface properties, such as activated carbon, carbon nanotubes (CNTs), carbon nanofibers (CNFs) and N-doped carbon nanofibers (N-CNFs), were utilized, whilst TiO_2 represents the oxide materials. Particular attention has been devoted to the impact of the impurities present in the raw glycerol on the activity and durability of the AuPd catalysts.

2. Results and Discussion

Raw glycerol was obtained from the transesterification of edible rapeseed vegetable oil. GC analysis revealed that the rapeseed vegetable oil was mainly composed of mono- and poly-unsaturated fatty acids; namely oleic acid (9-octadecenoic, C18:1), linoleic acid (9,12-octadecandienoic, C18:2), and the conjugated isomers thereof, and linolenic acid (9,12,15-octadecantrienoic, C18:3). Palmitic (hexadecanoic acid, C16:0) and stearic acids (octadecanoic acid, C18:0), saturated fatty acids, are in less quantity (Table 1).

Table 1. Typical fatty acid composition of rapeseed.

Oil	Fatty acids composition % by weight				
	C16:0	C18:0	C18:1	C18:2	C18:3
Rapeseed	4.39	1.94	63.93	20.67	9.07

The transesterification was carried out at 40 °C for 2 h using KOH as the base. At the end of the reaction, the glycerol solution was separated from the reaction media and used in the consecutive reactions without any pretreatment. Selective raw glycerol oxidation was performed using different AuPd bimetallic systems, supported on carbonaceous material or TiO_2 (glycerol 0.3 M, 50 °C, 3 atm O_2, glycerol/Au 1000 mol/mol, NaOH/glycerol 4 mol/mol). For understanding the importance of glycerol purity on the catalytic performance, a commercial grade glycerol was also studied under the same reaction conditions. AuPd catalysts were synthesized by impregnation of preformed metal nanoparticles using polyvinyl alcohol as a protective agent. We reported on a two-step procedure for the preparation of activated carbon-supported AuPd alloy nanoparticles (NPs) [24–26]. In this procedure, after immobilization of a preformed gold sol on activated carbon, a sol of palladium was generated in the presence of Au/AC using H_2 as the reducing agent. Herein, we extended this procedure to other supports (CNFs, N-CNFs, CNTs, TiO_2).

The resulting catalysts show a similar particle size for AuPd on AC, CNTs and N-CNFs (3.4, 3.5 and 3.7 nm for Au-Pd/AC, Au-Pd/CNTs and Au-Pd/N-CNFs, respectively) and are even distributed differently (Table 2). In the case of CNFs and TiO_2 as supports, bigger AuPd particles are measured

(4.5 and 4.1 nm for CNFs and TiO_2, respectively) (Table 2). As already highlighted in the literature, these results confirmed the beneficial effect of the presence of heteroatoms on the carbon nanofibers' surface in terms of stabilization of the metal nanoparticles with a better particle size distribution.

Table 2. Statistical median and standard deviation of 1% Au_6Pd_4 catalysts. AC, activated carbon; N-CNF, N-doped carbon nanofiber.

Catalyst	Statistical median (nm)	Standard deviation σ
1% Au_6Pd_4/CNFs	4.5	1.5
1% Au_6Pd_4/N-CNFs	3.7	0.9
1% Au_6Pd_4/CNTs	3.5	1.3
1% Au_6Pd_4/TiO_2	4.1	1.2
1% Au_6Pd_4/AC	3.4	0.7
1% Au_6Pd_4/AC after reaction using raw glycerol	4.6	1.2
1% Au_6Pd_4/AC after reaction using purified glycerol	3.5	0.7

In the case of AuPd on activated carbon, alloyed AuPd nanoparticles with a uniform composition and homogeneity were obtained [24–26]. In the other cases, most of the nanoparticles were alloyed, but the Au/Pd ratio was inhomogeneous from cluster to cluster. On the contrary, a partial segregation of Au and Pd was detected on 1% Au_6Pd_4/CNF, as evidenced by the elemental mapping (Figure 1).
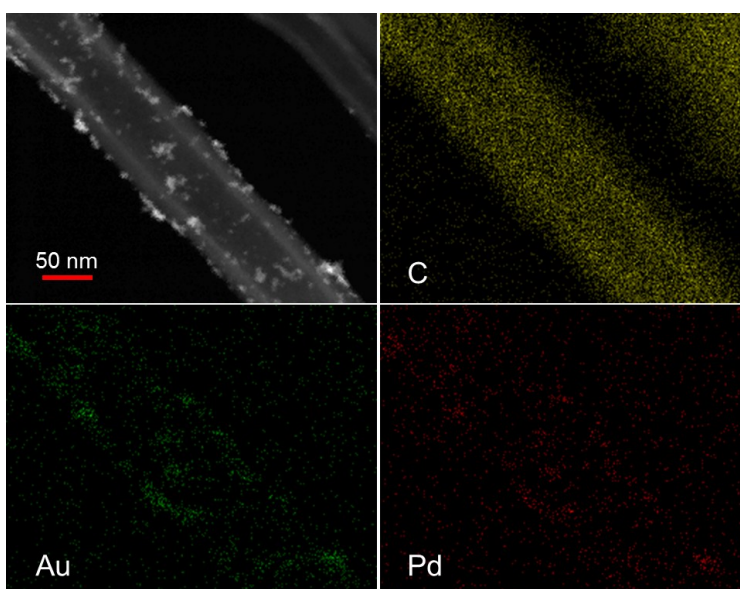

Figure 1. STEM image and element mapping on 1% Au_6Pd_4/CNF.

The catalysts were first tested in the oxidation of pure glycerol. The initial activity, expressed as mol of glycerol converted per mol of metal per hour, calculated at 15 min of reaction, as well as a selectivity at 90% conversion are reported in Table 3. One percent Au_6Pd_4/AC resulted in the most active catalysts with an initial activity (3205 mol/mol h) at least three-times more active than 1% Au_6Pd_4/N-CNFs (1076 mol/mol h) and 1% Au_6Pd_4/CNTs (815 mol/mol h), despite a similar AuPd particle size (3.4–3.7 nm). This result is in agreement with the findings that AuPd homogeneous alloys are more active than inhomogeneous phases in the alcohol oxidation due to a synergistic effect [24–26,29]. One percent

Au_6Pd_4/CNFs and 1% Au_6Pd_4/TiO_2 resulted in less activity (675 and 628 mol/mol h, respectively), probably due the presence of bigger particle sizes (4.5 and 4.1 nm) (Table 2).

The selectivity to glyceric acid is slightly higher for 1% Au_6Pd_4/CNFs and 1% Au_6Pd_4/TiO_2 (78–79%) compared to the one of 1% Au_6Pd_4/CNTs (70%) (Table 3). This trend can be explained by observing the AuPd particle sizes (4.5, 4.1 and 3.5 nm, for Au_6Pd_4 supported on CNFs, TiO_2 and CNTs, respectively). Indeed, it has been reported that the metal nanoparticle size is one of the factors influencing the selectivity in glycerol oxidation, with larger particles giving higher selectivity towards glyceric acid [8–15].

Table 3. Glycerol oxidation over 1% Au_6Pd_4-based carbon and oxide supports. Glycerol was obtained from the transesterification of rapeseed oil. Reaction conditions: glycerol, 0.3 M; substrate/total metal = 1000 mol/mol; total volume, 10 mL; 4 eq NaOH; 50 °C; 3 atm O_2.

Origin of glycerol	Catalyst	Initial activity [a]	Selectivity (%) [b]		
			Glyceric acid	Tartronic acid	C1 + C2 product
Pure glycerol	1% Au_6Pd_4/AC	3205	77	5	14
	1% Au_6Pd_4/N-CNFs	1076	66	22	8
	1% Au_6Pd_4/CNTs	815	70	8	10
	1% Au_6Pd_4/CNFs	675	78	11	9
	1% Au_6Pd_4/TiO_2	628	79	8	12
Raw glycerol	1% Au_6Pd_4/AC	1672	72	15	11
	1% Au_6Pd_4/N-CNFs	736	71	17	10
	1% Au_6Pd_4/CNTs	651	72	15	12
	1% Au_6Pd_4/CNFs	269	81	8	10
	1% Au_6Pd_4/TiO_2	230	78	10	10
Purified raw glycerol	1% Au_6Pd_4/AC	3150	75	7	15
	1% Au_6Pd_4/TiO_2	598	79	3	14
Pure glycerol + fatty acids	1% Au_6Pd_4/AC	1523	73	14	13
	1% Au_6Pd_4/TiO_2	185	79	5	16

[a] Glycerol converted moles per hour per mole of metal, calculated after 15 min of reaction; [b] selectivity calculated at 90% conversion.

On the other hand, 1% Au_6Pd_4/AC showed a comparable selectivity as 1% Au_6Pd_4/CNFs and 1% Au_6Pd_4/TiO_2 (77–79%) despite smaller AuPd particle sizes (3.5, 4.1 and 4.5 nm for AuPd on AC, TiO_2 and CNFs, respectively). This result can be justified by the better selectivity to glyceric acid evidenced in the presence of the pure AuPd alloy, instead of the inhomogeneous phases [24–26]. One percent Au_6Pd_4/N-CNFs showed the lowest selectivity to glyceric acid (66%) with the formation of a high amount of tartronic acid, which is the product of the consecutive reaction of glycerol to tartronate. Probably the presence of nitrogen groups altered the AuPd active sites by an electronic effect, promoting the overoxidation reaction.

The same catalysts have been tested using raw instead of pure glycerol. All of the catalysts resulted in less activity, but following the same order as when tested in pure glycerol: AC > N-CNFs > CNTs > CNFs > TiO_2. We attributed the lower activity to the presence of impurities that adsorbed onto the AuPd catalysts, partially blocking the active sites. In order to prove this

hypothesis, the raw glycerol was purified from the impurities derived from the transesterification process. This process consists first in the addition of H_2SO_4 to the glycerol solution to convert the soap into free fatty acid. Therefore, free fatty acids were removed by extraction with hexane, and then, methanol was removed by evaporation. The glycerol solution was then separated and treated with activated carbon in order to remove free ions. Lastly, the activated carbon was separated by filtration.

The most active 1% Au_6Pd_4/AC and the less active 1% Au_6Pd_4/TiO_2 catalysts were tested with the purified glycerol. Similar results as the one obtained with commercial pure glycerol on both catalysts were obtained. Finally, the same catalysts have been tested, adding rapeseed oil (10 wt% with respect to glycerol) to pure glycerol (Table 3). The results highlighted that the addition of fatty acid to pure glycerol has a detrimental effect on the activity, with an initial activity even lower than the one obtained using raw glycerol. Figure 2 reported the conversion/time curves using 1% Au_6Pd_4/AC and 1% Au_6Pd_4/TiO_2, clearly showing that the reaction profile is strongly influenced by the type of glycerol. Indeed, in the presence of pure or purified glycerol, full conversion was obtained after 1 h, whereas in the presence of fatty acids, a lower activity was observed, possibly due to the blocking of some active sites by the adsorbed species.
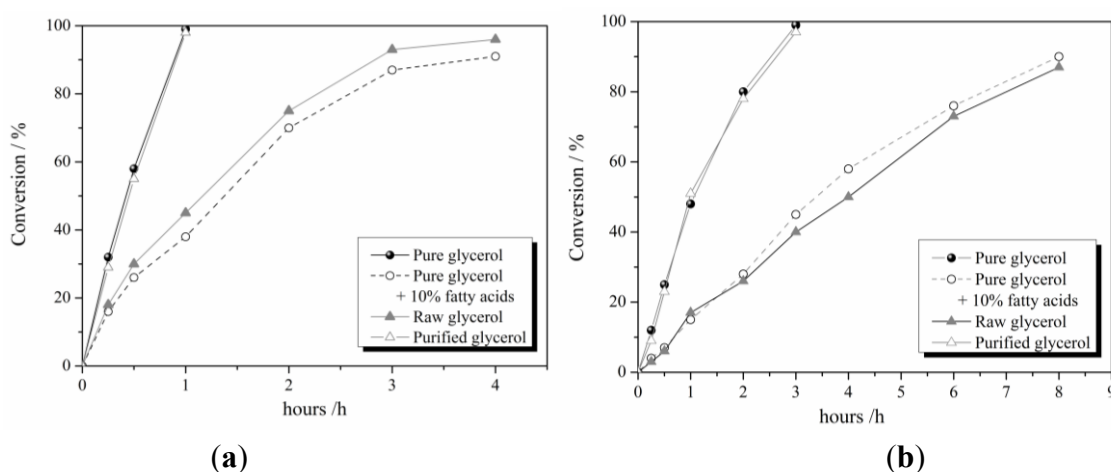

Figure 2. Reaction profile for pure glycerol, pure glycerol + 10% fatty acid, raw glycerol and purified glycerol using (**a**) 1% Au_6Pd_4/AC and (**b**) 1% Au_6Pd_4/TiO_2.

To investigate in more detail this latter finding, Fourier transform infrared spectroscopy studies were carried out on 1% Au_6Pd_4/TiO_2 after reaction with both raw and pure glycerol. Figure 3 shows the recorded IR spectra of the used catalysts after reaction using pure and raw glycerol. In the case of glycerol derived from the transesterification of rapeseed oil, the bands at 2921 and 2846 cm^{-1} were assigned to the sp^3 asymmetric CH_2 stretch and the symmetric CH_2 stretch, respectively. The band at 2959 cm^{-1} was attributed to the sp^2 C-H stretch in C=C-H, highlighting thus the presence of C=C. The assignment of these three bands are in agreement with Wu *et al.* [30]. Moreover, a conjugated ν(C=C) stretch is highlighted by the bands at 1638 and 1595 cm^{-1}. The presence of these carbon double bonds could be explained by the presence of some traces of oleic, linoleic and linolenic acids in the raw glycerol. Probably, these unsaturated species were adsorbed on the catalyst during the glycerol oxidation. Indeed, these species are not present in the IR spectrum of the catalyst used for the selective pure glycerol oxidation

(Figure 3). The bands in common between the pure and the raw glycerol are at 1456 and 1402 cm^{-1} and were attributed to O-H in plane [30] and to C-O-H bending vibration [31], respectively.

This finding can be extended to the carbon-based AuPd catalyst. However, the nature of the support makes investigation using infrared spectroscopy more difficult. The characteristic band of C=C at 2959 cm^{-1} and the one at 1638–1595 cm^{-1}, attributed to the conjugated C=C, are due to the presence in the raw glycerol of some fatty acids. These long unsaturated chains could easily block access to the active sites, as already reported by Gil *et al.* [16,17]. They indeed ascribed the decrease of the catalytic activity when using crude glycerol as the feedstock with the presence of impurities, namely the methyl esters. The latter produce important changes in the surfaces properties of the support and the leaching of gold into the liquid reaction solution. During the phase separation after the transesterification, despite all care being taken, it becomes obvious that traces of the fatty acids were mixed together with the co-product, glycerol.
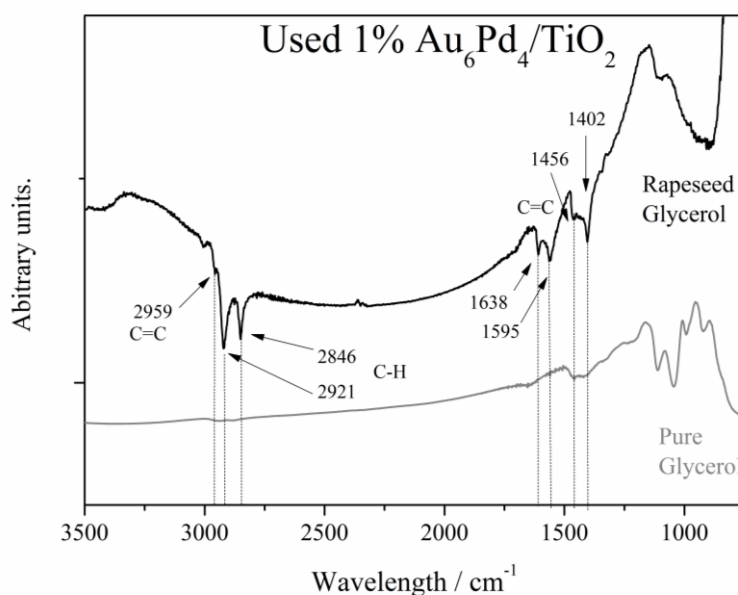

Figure 3. FT-IR spectra of the used 1% Au$_6$Pd$_4$/TiO$_2$ after glycerol oxidation. Reaction conditions: glycerol, 0.3 M; substrate/total metal = 1000 mol/mol; total volume, 10 mL; 4 eq NaOH; 50 °C; 3 atm O$_2$.

The effect of the nature of the glycerol on the durability of the catalyst was evaluated by a recycling test using the most active catalyst, 1% Au$_6$Pd$_4$/AC. Recycling experiments were carried out just by filtering the catalyst and adding a fresh solution of glycerol using purified and non-purified raw glycerol (Figure 4).

Figure 4 shows that, when the glycerol was not formerly purified, the activity of the 1% Au$_6$Pd$_4$/AC catalyst rapidly decreases, while the selectivity to glyceric acid increase. Indeed, from Run 1 to Run 8, a drop of conversion (from 89% to 6%) occurred. Along the eight successive reactions, the selectivity to glyceric acid is constantly increasing (from 77% to 87%). Such an increase in the value of the selectivity suggests an increase of the bimetallic AuPd particle size. This assumption is confirmed by measuring the mean particle size of the AuPd on the used catalysts with an increase from 3.4 to 4.7 nm (Table 2), with the presence of aggregated AuPd particles in some regions (Figure 5).

On the contrary, the conversion (about 94%), as well as the selectivity to glyceric acid (around 77%) remained constant over the eight runs using the purified glycerol (Figure 4). TEM investigation confirmed that the morphology of the AuPd nanoparticles was not significantly modified during the stability test, with AuPd mean sizes of 3.4 and 3.5 nm before and after the reaction, respectively (Table 2).

The impact of the purity of the glycerol on the stability of the catalyst was confirmed by analyzing the leaching of metal in both cases. Moreover, ICP analyses of the collected solution of the eight runs resulted in a loss of 15 wt% of total metal in the case of non-purified glycerol against only 1% in the case of the purified one.
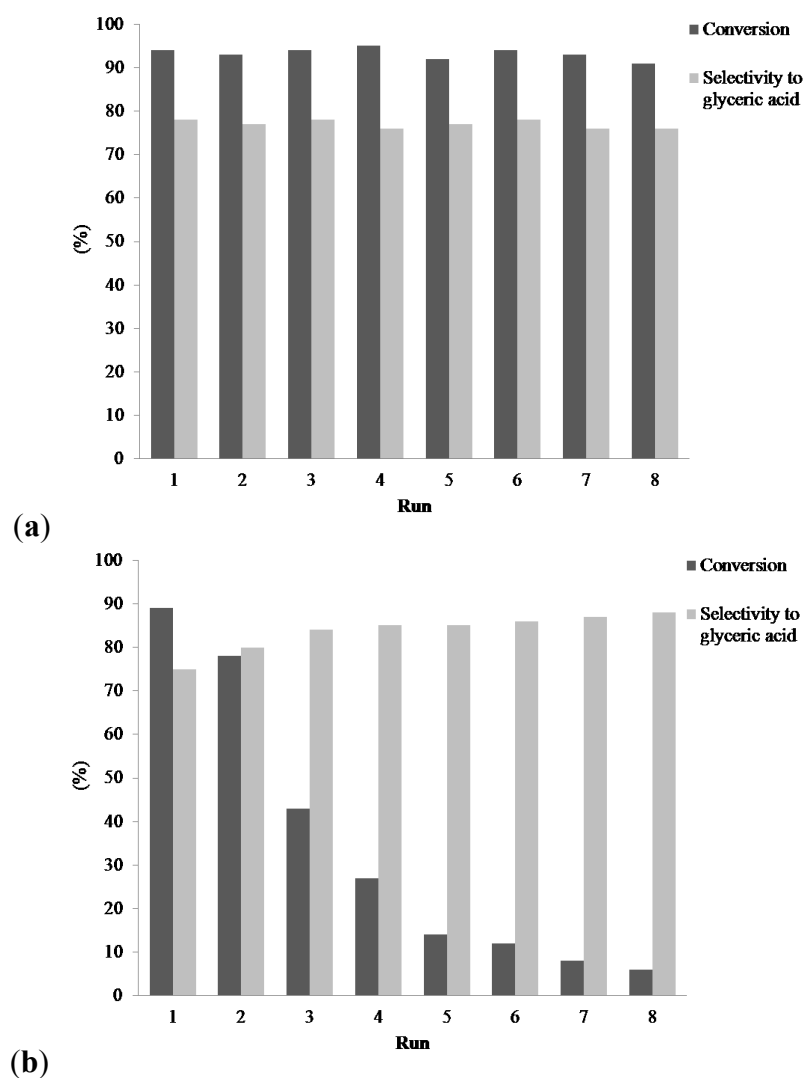

(**a**)

(**b**)

Figure 4. Evolution of the glycerol conversion over 1% Au_6Pd_4/AC and over the eight runs using (**a**) the purified glycerol and (**b**) the non-purified glycerol directly obtained from transesterification of rapeseed oil. Reaction conditions: glycerol, 0.3 M; substrate/total metal = 1000 mol/mol; total volume, 10 mL; 4 eq NaOH; 50 °C; 3 atm O_2.
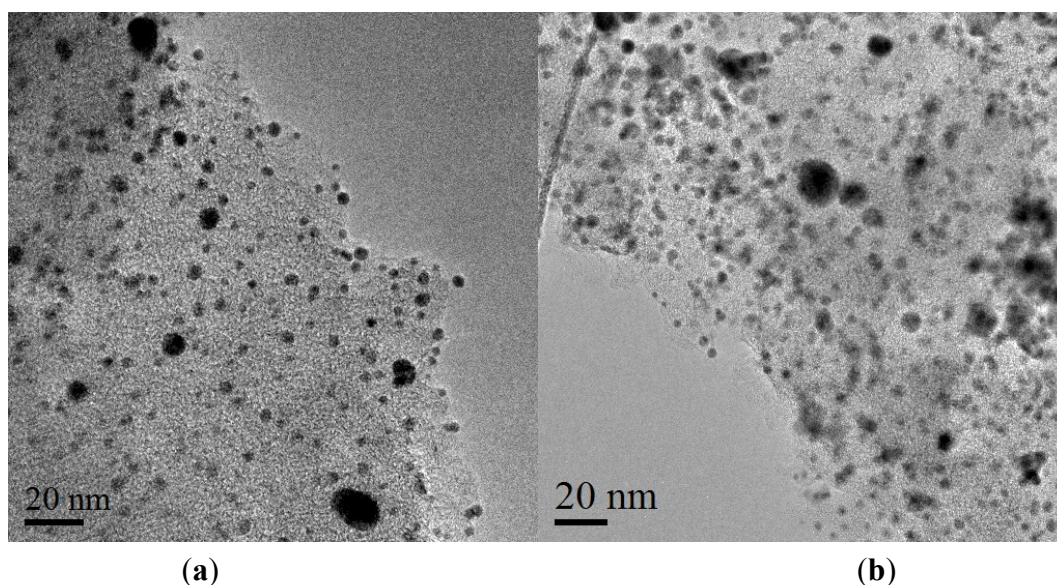
Figure 5. TEM images of AuPd/AC (**a**) before and (**b**) after the recycling tests using raw glycerol.

3. Experimental Section

3.1. Materials

Fatty acid methyl esters (FAMEs) and, therefore, the by-product, raw glycerol, were obtained by the homogeneous transesterification of rapeseed oil with methanol (MeOH:triglycerides = 6:1 mol/mol) and KOH (1% by weight) as the catalyst. This mixture was magnetically stirred for two hours at 40 °C. After the reaction, by simple decantation methyl esters are separated from the raw glycerol. The final methyl ester was obtained after removing the excess of alcohol under vacuum and a final filtration on silica powder. In the case of non-purified raw glycerol, the glycerol was used as obtained.

Glycerol (87 wt% solution), glyceric acid and tartronic acid were purchased from Fluka. $NaAuCl_4$ $2H_2O$ and Na_2PdCl_4 were from Aldrich (99.99% purity), activated carbon from Camel (X40S; SA = 900–1100 m^2/g; PV = 1.5 mL/g; pH 9–10), commercial carbon nanotubes, Baytubes (average diameter of 10 ± 2 nm and a specific surface area of 288 m^2/g), from Bayer, commercial CNFs PR24-PS from Applied Science (average diameter of 88 ± 30 nm and a specific surface area of 43 m^2/g) and the 3% *N*-containing CNFs from the pre-oxidized CNFs by thermal treatment (10 g) with NH_3 at 600 °C for 4 h, as reported in [32]. TiO_2 (P25) was purchased from Degussa (SA = 50 m^2/g). $NaBH_4$ of purity >96% from Fluka and polyvinyl alcohol (PVA) (M_w = 13,000–23,000 87–89% hydrolysed) from Aldrich were used. Gaseous oxygen from SIAD was 99.99% pure.

3.2. Catalyst Preparation

1% Au_6Pd_4 Bimetallic Catalysts

$NaAuCl_4$ $2H_2O$ (0.072 mmol) was dissolved in 140 mL of H_2O, and PVA (2% *w/w*) was added (0.706 mL). The yellow solution was stirred for 3 minutes, and 0.1 M $NaBH_4$ (2.15 mL) was added under vigorous magnetic stirring. The ruby red Au(0) sol was immediately formed. A UV-visible spectrum of the gold sol was recorded to check the complete $AuCl_4^-$ reduction and the formation of the

plasmon peak. Within a few minutes of sol generation, the gold sol (acidified until pH 2 by sulfuric acid) was immobilized by adding the support under vigorous stirring. The amount of support was calculated as having a final metal loading of 0.73 wt%. After 2 h, the slurry was filtered and the catalyst washed thoroughly with distilled water (neutral mother liquors). A check of Au loading was performed directly on the catalysts, confirming the quantitative adsorption of Au NPs of the sol. The Au/support was then dispersed in 140 mL of water; Na_2PdCl_4 (10 wt% in Pd solution) (0.0386 mL) and PVA (2% *w/w*) (0.225 mL) were added. H_2 was bubbled (50 mL/min) under atmospheric pressure and room temperature for 2 h. The slurry was filtered and the catalyst washed thoroughly with distilled water. The total metal loading of 1 wt% and the Au-Pd molar ratio 6:4 was confirmed by ICP analyses for all of the catalysts. The catalysts were labeled as 1% Au_6Pd_4/AC, 1% Au_6Pd_4/N-CNFs, 1% Au_6Pd_4/CNTs, 1% Au_6Pd_4/CNFs and 1% Au_6Pd_4/TiO$_2$.

3.3. Catalytic Tests

Glycerol was obtained as a by-product by traditional transesterification starting from a commercial and edible rapeseed vegetable oil and using KOH as the base. The composition of the rapeseed oil was completed by GC using a HP 7820A gas chromatograph equipped with a non-bonded, bis-cyanopropyl polysiloxane (100 m) capillary column. The homogeneous transesterification of the rapeseed oil was carried out at 40 °C for two hours, as described in this section.

To obtain a purified glycerol, the resulted glycerol solution was diluted in a ratio of 1/10 in order to reduce the fluid viscosity and used as obtained or further purified. In the latter case, H_2SO_4 was added in order to adjust the pH to 2 and to convert the soap into free fatty acid. The free fatty acid was removed by extraction with hexane. The obtained methanol-glycerol mixture was evaporated in a rotavapor in order to remove the methanol. The glycerol solution was then separated and treated with activated carbon in order to remove the free ions. The activated carbon was separated by filtration. Finally, the glycerol solution was diluted with water in order to obtain the desired concentration (0.3 M). The presence of possible impurities was verified using high-performance liquid chromatography (HPLC) using a column (Alltech OA-10308, 300 mm × 7.8 mm) with UV and refractive index (RI) detection or GC using an HP 7820A gas chromatograph equipped with a capillary column (HP-5 30 m × 0.32 mm, 0.25 μm film, by Agilent Technologies)) and a TCD detector. GC-MS was used for the identification of the products.

Glycerol oxidation: reactions were carried out in a 30-mL glass reactor equipped with a thermostat and an electronically-controlled magnetic stirrer connected to a 5000-mL reservoir charged with oxygen (3 atm). The oxygen uptake was followed by a mass-flow controller connected to a PC through an A/D board, plotting a flow time diagram.

Glycerol 0.3 M and the catalyst (substrate/total metal = 1000 mol/mol) were mixed in distilled water (total volume, 10 mL) and 4 equivalents of NaOH. The reactor was pressurized at 3 atm of oxygen and set to 50 °C. Once this temperature was reached, the gas supply was switched to oxygen, and the monitoring of the reaction started. The reaction was initiated by stirring. Recycling tests were carried out under the same conditions (substrate/total metal = 1000 mol/mol, 50 °C, 3 atm O_2, 1250 rpm, alcohol 0.3 M, 1 h for purified and 3 h for non-purified glycerol). A test was performed adding to a 0.3 M solution of pure glycerol 10 wt% of fatty acids (rapeseed).

The catalyst was recycled in the subsequent run after filtration without any further treatment. Samples were removed periodically and analyzed by high-performance liquid chromatography (HPLC) using a column (Alltech OA- 10308, 300 mm × 7.8 mm) with UV and refractive index (RI) detection to analyze the mixture of the samples. Aqueous H_3PO_4 solution (0.1 wt%) was used as the eluent. Products were identified by comparison with the original samples.

3.4. Characterization

3.4.1. Catalyst Characterization

(1) The metal content was checked by ICP analysis of the filtrate or, alternatively, directly on the catalyst after burning off the carbon, on a Jobin Yvon JY24.

(2) The morphology and microstructures of the catalysts were characterized by transmission electron microscopy (TEM). The powder samples of the catalysts were ultrasonically dispersed in ethanol and mounted onto copper grids covered with holey carbon film. A Philips CM200 FEG electron microscope, operating at 200 kV and equipped with an EDX DX4 analyzer system and a FEI Titan 80-300 electron microscope, operating at 300 kV and equipped with an EDX SUTW detector, were used for TEM observation.

(3) Fourier transform infrared (FT-IR) spectra were recorded with a JASCO FT/IR 410 spectrometer using a mercury cadmium telluride (MCT) detector. Spectra with 4 cm^{-1} resolution, 64 scans and a scan speed of 0.20 cm s^{-1} were recorded at room temperature using KRS5 thallium bromo-iodide windows in the range 4000–1000 cm^{-1}. The 1% Au_6Pd_4/TiO_2 used, which was filtered and dried after the reaction, was mixed with KBr to obtain a pellet (pressed at 10 MPa for 10 minutes).

4. Conclusions

One percent Au_6Pd_4 nanoparticles deposited on different supports were investigated in pure and raw glycerol. We addressed the best catalytic performance of 1% Au_6Pd_4/AC in the presence of uniform alloy AuPd nanoparticles. Indeed, in the other cases, inhomogeneity in the AuPd composition, together with the partial segregation of Au and Pd, was detected. A general decrease in activity was observed when raw glycerol was used as the substrate. FT-IR results revealed the presence of traces of unsaturated fatty acids on the catalyst surface. These unsaturated compounds probably partially blocked the AuPd active sites, decreasing the activity. The effect of the nature of the glycerol was investigated on the durability of 1% Au_6Pd_4/AC. A strong deactivation was observed in the presence of non-purified glycerol due to the agglomeration and leaching of the metal nanoparticles. On the contrary, the catalyst showed a good stability when purified glycerol was used.

Author Contributions

Carine E. Chan-Thaw made the catalytic tests and worked on the redaction of the article. Sebastiano Campisi performed some additional catalytic tests. Di Wang made the TEM and EDX analysis. Laura Prati contributed by overviewing the manuscript, and finally, Alberto Villa synthesized the catalysts and overviewed the article.

Conflicts of Interest

The authors declare no conflict of interest.

Acknowledgements

References

1. Zhou, C.-H.; Beltramini, J.N.; Fan, Y.-X.; Lu, G.Q. Chemoselective catalytic conversion of glycerol as a biorenewable source to valuable commodity chemicals. *Chem. Soc. Rev.* **2008**, *37*, 527–549.

2. Lawate, S.S.; Lal, K. High oleic polyol esters, compositions and lubricants functional fluids and greases containing the same. European Patent 0712834A1, November, 1994.

3. Heidbreder, A.; Gruetzmacher, R.; Nagorny, U.; Westfechtel, A. Use of fatty ester-based polyols for polyurethane casting resins and coating materials. US Patent 2002/0161161 A1, October, 2002.

4. Gallezot, P. Conversion of biomass to selected chemical products. *Chem. Soc. Rev.* **2012**, *41*, 1538–1558.

5. Mittelbach, M.; Remschmidt, C. *Biodiesel: The Comprehensive Handbook*; Boersedruck Ges M.B.H.: Vienna, Austria, 2004.

6. McCoy, M. Glycerin surplus. *Chem. Eng. News* **2006**, *84*, 7–8.

7. Gu, Y.; Jérôme, F. Glycerol as a sustainable solvent for green chemistry. *Green Chem.* **2010**, *12*, 1127–1138.

8. Carrettin, S.; McMorn, P.; Johnston, P.; Griffin, K.; Kiely, C.J.; Hutchings, G.J. Oxidation of glycerol using supported Pt, Pd and Au catalysts. *Phys. Chem. Chem. Phys.* **2003**, *5*, 1329–1336.

9. Porta, F.; Prati, L. Selective oxidation of glycerol to sodium glycerate with gold-on-carbon catalyst: an insight into reaction selectivity. *J. Catal.* **2004**, *224*, 397–403.

10. Demirel-Gülen, S.; Lucas, M.; Claus, P. Liquid phase oxidation of glycerol over carbon supported gold catalysts. *Catal. Today* **2005**, *102*, 166–172.

11. Dimitratos, N.; Villa, A.; Bianchi, C.L.; Prati, L.; Makkee, M. Gold on Titania: Effect of preparation method in the liquid phase oxidation. *Appl. Catal. A* **2006**, *311*, 185–192.

12. Dimitratos, N.; Villa, A.; Prati, L. Liquid Phase Oxidation of glycerol using a single phase (Au–Pd) alloy supported on activated carbon: Effect of reaction conditions. *Catal. Lett.* **2009**, *133*, 334–340.

13. Villa, A.; Wang, D.; Su, D.S.; Prati, L. Gold sols as catalysts for glycerol oxidation: The role of stabilizer. *ChemCatChem* **2009**, *1*, 510–514.

14. Chan-Thaw, C.E.; Villa, A.; Katekomol, P.; Su, D.; Thomas, A.; Prati, L. Covalent triazine framework as support for liquid phase reaction. *Nano Lett.* **2010**, *10*, 537– 541.

15. Villa, A.; Veith, G.M.; Prati, L. Selective Oxidation of glycerol under acidic conditions using gold Catalysts. *Angew. Chem. Int. Ed*. **2010**, *49*, 4499–4502.

16. Gil, S.; Marchena, M.; Sánchez-Silva, L.; Sánchez, P.; Romero, A.; Valverde, J.L. Effect of the operation conditions on the selective oxidation of glycerol with catalysts based on Au supported on carbonaceous materials. *Chem. Eng. J.* **2011**, *178*, 423–435.

17. Gil, S.; Marchena, M.; María Fernández, C.; Sánchez-Silva, L.; Romero, A.; Valverde, J.L. Catalytic oxidation of crude glycerol using catalysts based on Au supported on carbonaceous materials. *Appl. Catal. A* **2013**, *450*, 189– 203.

18. Skrzyńska, E.; Wondołowska-Grabowska, A.; Capron, M.; Dumeignil, F. Crude glycerol as a raw material for the liquid phase oxidation reaction. *Appl. Catal. A* **2014**, *482*, 245– 257.

19. Konaka, A.; Tago, T.; Yoshikawa, T.; Nakamura, A.; Masuda, T. Conversion of glycerol into allyl alcohol over potassium-supported zirconia–iron oxide catalyst. *Appl. Catal. B* **2014**, *146*, 267–273.

20. Krähling, L.; Krey, J.; Jakobson, G.; Grolig, J.; Miksche, L. Allyl Compounds. In *Ullmann's Encyclopedia of Industrial Chemistry*; Wiley-VCH Verlag GmbH & Co. KGaA: Weinheim, Germany, 2000.

21. Corma, A.; Garcia, H. Supported gold nanoparticles as catalysts for organic reactions. *Chem. Soc. Rev.* **2008**, *37*, 2096–2126;

22. Della Pina, C.; Falletta, E.; Prati, L.; Rossi, M. Selective oxidation using gold. *Chem. Soc. Rev.* **2008**, *37*, 2077–2095;

23. Besson, M.; Gallezot, P. Selective oxidation of alcohols and aldehydes on metal catalysts. *Catal. Today* **2000**, *57*, 127–141.

24. Wang, D.; Villa, A.; Porta, F.; Su, D.; Prati, L. Single-Phase Bimetallic System for the Selective Oxidation of Glycerol to Glycerate. *Chem.Comm.* **2006**, *18*, 1956–1958.

25. Villa, A.; Campione, C.; Prati, L. Bimetallic gold/palladium catalysts for the selective liquid phase oxidation of glycerol. *Catal. Lett.* **2007**, *115*, 133–136.

26. Wang, D.; Villa, A.; Porta, F.; Prati, L.; Su, D. Bimetallic Gold/Palladium Catalysts: Correlation between Nanostructure and Synergistic Effects. *J. Phys. Chem. C* **2008**, *112*, 8617–8622.

27. Prati, L.; Villa, A.; Chan-Thaw, C.E.; Arrigo, R.; Wang, D.; Su, D.S. Gold catalyzed liquid phase oxidation of alcohol: the issue of selectivity. *Faraday Discuss.* **2011**, *152*, 353–365.

28. Prati, L.; Villa, A.; Lupini, A.R.; Veith, G.M. Gold on carbon. One billion catalysts under a single label. *Phys. Chem. Chem. Phys.* **2012**, *14*, 2969–2978.

29. Prati, L.; Villa, A.; Porta, F.; Wang, D.; Su, D.S. Single-phase gold/palladium catalyst: The nature of synergistic effect. *Catal. Today* **2007**, *122*, 386 – 390.

30. Wu, N.; Fu, L.; Su, M.; Aslam, M.; Chun Wong, K.; Dravid, V.P. Interaction of fatty acid monolayers with cobalt nanoparticles. *Nano Lett.* **2004**, *4*, 383–386.

31. Nor Hidawati, E.; Mimi Sakinah, A.M. Treatment of glycerin pitch from biodiesel production. *Int. J. Chem. Environ. Eng.* **2011**, *2*, 309–313.

32. Arrigo, R.; Haevecker, M.; Wrabetz, S.; Blume, R.; Lerch, M.; McGregor, J.; Parrott, E.P.J.; Zeitler, J.A.; Gladden, L.F.; Knop-Gericke, A.; Schloegl, R.; Su, D. Tuning the acid/base properties of nanocarbon by functionalization via amination. *J. Am. Chem. Soc.* **2010**, *132*, 9616–9630.